Proceedings of the Twenty-fourth (2014) International Ocean and Polar Engineering Conference **www.isope.org**
Busan, Korea, June 15-20, 2014

ISBN 978-1 880653 91-3 (Set); ISSN 1098-6189 (Set)

Updating Fatigue Reliability of Uninspectable Joints using Structurally Correlated Inspection Data

David van den Berg (1), *Mark Tammer* (2) and *Miroslaw Lech Kaminski* (3)

(1) Ship Hydromechanics and Structures, Maritime and Transport Technology, Faculty of Mechanical, Maritime and Materials Engineering, Delft University of Technology (TU-Delft), The Netherlands.
(2)Institute for Engineering & Design, Faculty of Natural Sciences and Technology, HU University of Applied Sciences Utrecht, The Netherlands.
(3) Ship Hydromechanics and Structures, Maritime and Transport Technology, Faculty of Mechanical, Maritime and Materials Engineering, Delft University of Technology (TU-Delft), The Netherlands.

ABSTRACT

This paper outlines an investigation into the updating of fatigue reliability through inspection data by means of structural correlation. The proposed methodology is based on the random nature of fatigue fracture growth and the probability of damage detection and introduces a direct link between predicted crack size and inspection results. A distinct focus is applied on opportunities for utilizing inspection information for the updating of both inspected and uninspected (or uninspectable) locations.

KEY WORDS: Structural Longevity; Fatigue Reliability; Fracture Mechanics (FM); Risk Based Inspection (RBI).

INTRODUCTION

Among the many degradation mechanisms that are influencing the structural longevity of ship and offshore structures, fatigue is the primary cause of the majority of structural failures (Lemaitre and Desmorat, 2005). The highly stochastic nature of this process has provided lots of models and inherent uncertainties, which emphasize a probabilistic foundation. Despite considerable developments in both structural reliability theory and computational methods, the probabilistic approach has gained little ground on the deterministic approach. As a consequence, most operators of ship and offshore structures base decisions regarding Inspection, Repair and Maintenance efforts on empirical procedures. The lack of acceptance of probabilistic methods for assessment of fatigue fracture deterioration may be assigned to the complexity and computational effort concerned with the approach, and the long absence of research into practical applications.

Hence, in operation, structural inspection practices are deployed as the key instrument to assess the actual asset integrity by identification and mitigation of system anomalies and unanticipated defects to ensure structural longevity and an adequate level of safety to comply with statuary rules and company guidelines. With this in mind, the historic perspective of inspections is logically based on empirical findings. In general, the assessment of fatigue-prone structural locations (hot-spots) is performed by the application of the S-N approach.

The direct incorporation of the crack inspection results is challenging, as the definition of damage cannot be directly related to detected crack size. Therefore, the Fracture Mechanics-methodology is deployed as the de-facto standard to relate the number of stress cycles to the crack size.

After gaining experience from the initial and subsequent inspections, asset specific degradation patterns for probabilistic models can be constructed to produce estimations about asset degradation and structural integrity at a specific time in the future. By linking this understanding of degradation propagation with the classification of the inherent risks of this process and the consequences of failure, a more specific assessment and risk ranking can be made as an alternative for prescriptive practices - which could be unsuitable for a specific asset design and/or operational context (over- or under stringent). This practice is referred to as Risk Based Inspection (RBI) (Tammer and Kaminski, 2013) and is becoming a more popular practise and noticeable adopted by all major inspection and classification bodies. In RBI, the information about the existence or non-existence of damage provides information, which can be used to update the deterioration model of a structure to reduce uncertainty, direct efforts to specific locations and details and may result in a change of inspection methods or intervals. At this moment, RBI efforts are often limited to single components or (sub)assemblies and disregards systems effects.

The outcome of the inspection and hence quality of the information gained is limited by the Probability of Detection (PoD), which is influenced by the deployed methodology, circumstances and human factors) and the inspectability of details due to limitations in e.g. accessibility or technological restrains. However, as details are likely to share characteristics and parameters in materials, design and fabrication, loading mechanisms and operational context, the degradation correlation can be distinct. With knowledge about these relations, the inspection information about one particular structural component may be linked to other parts of the structure. In this way, inspection information can by fully utilized, not only for inspected components, but also for uninspected parts of the structure (Moan and Song, 2000). Although the importance of structural correlation has been emphasized upon, efforts into including the correlation effect in system fatigue deterioration modelling has been very limited.

In order to provide a clear picture, the state of the art knowledge in fatigue deterioration and reliability analysis is discussed. A single component fatigue fracture model is set up and investigated for several inspection scenarios and extended to a multiple component model where structural correlation is introduced. Subsequently, it is concluded that the use of structural correlation in system reliability updating enhances the efficient and effective use of system inspection information.

Inspection Modelling

Reformulation of the Paris law shows the relation between the number of stress cycles and the related fatigue fracture and is used to derive a limit state model $M(x,t)$ for fatigue fracture crack growth. This is depicted as a function of the vector of random variables $\mathbb{x} = [\mathrm{a}_o, \mathrm{a}_c, C, m, S]T$ and time. The first term on the right hand side of Equation 1 depends on fatigue and material characteristics and therefore describes the fatigue strength. The second term represents the fatigue loading:

$$M(\mathbb{x},t) = \int_{a_0}^{a_c} \frac{da}{(Y(a)\sqrt{\pi a})^m} - \int_0^N CS^m \, dN \qquad [1]$$

The Probability of Failure *(PoF)* of a component given a duration t is described by the probability of $M(\mathbb{x},t) \leq 0$. Since the focus of this paper is on reliability methods and not on fracture mechanics of structural details, the DNV (1995) two-parameter Weibull distribution for the description of the expected value of the stress is used, with A and B as the scale and shape parameters:

$$\sum_{i=1}^{N} S_i^m = \nu_0 t A^m \Gamma\left(1+\frac{m}{B}\right) \qquad [2]$$

The level of uncertainty associated with the initial limit state can be reduced with evidence about the (non-)existence of fatigue fractures found during Inspection Events (IE). By applying conditional probability, the *PoF* can be updated and (no-)repair decisions made. At this moment, the de-facto standard consists of visual inspection complemented with Non-Destructive Testing - with a specific application and inherent Probability of Detection. Crack detection can be described similar to Equation 1. When measured, the load part of the limit state is equal to the resistance integral, integrated to the measured crack length:

$$IE_d(\mathbb{x},T_m) = \int_{a_0}^{a_m} \frac{da}{(Y(a)\sqrt{\pi a})^m} - C\nu_0 T_m A^m \Gamma\left(1+\frac{m}{B}\right) = 0 \qquad [3]$$

Measurements of a can be regarded as another random variable, since the accuracy of the measurement method introduces inherent uncertainty. If the detected fracture is repaired, the initial crack size a_o has to be replaced with a new random variable representing the initial fracture size related to the repair method (Moan and Song, 2000). If no detections are made during an inspection, two options are possible: either no crack exists, or it is too small to be detected. Similar to Equation 3 the inspection event of no crack detection is described by:

$$IE_{nd}(\mathbb{x},T_{in}) = \int_{a_0}^{a_d} \frac{da}{(Y(a)\sqrt{\pi a})^m} - C\nu_0 T_{in} A^m \Gamma\left(1+\frac{m}{B}\right) = 0 \qquad [4]$$

Here, the detectable crack size $\mathrm{a_d}$ is a random variable as well. An exponential distribution is most commonly used to model the PoD, which is influenced by the methods, procedures and instruments deployed. This is referred to in HSE OTR 2000/018 (HSE, 2002), the ICON database (1996), the BS7910 and other references and experiences gained. In addition, the work by Demsetz and Cabrera (1999) for the SSC-40 shows the factors and limitations of human inspection.

If no cracks are detected, the updating can be performed with the original fatigue limit state. If repair actions are initiated, the physical changes need to be accounted for in the limit state formulations, as the statistical properties of the material change. Commonly, the repair involves grinding of the crack; the new material variables ($\mathrm{a_r}$, $\mathrm{C_r}$ and $\mathrm{m_r}$) are modelled with the same properties as the original ($\mathrm{a_o}$, C and m), but are statistically independent (Moan and Song, 2000). If a crack is detected, but no repairs are made, the original limit state changes as well. The measured crack size can be used to reset the original limit state with a new initial crack size, and the time corrected for the moment of the measurement of the crack.

The initial crack size distribution is obtained from Moan et al (1997). The post repair variable a_r follows the same distribution, but is independent from a_o. The Paris law parameters and load variables follow the values of Moan and Song (2000). Geometry function parameters Y_1 and Y_2 are consistent with Jiao & Moan (1990) and Madsen et al. (1987). Stress intensity threshold ΔK_{th} is taken as 0. It is recognised that neglect of the threshold effect will result in conservative reliability predictions. The number of stress cycles per year, ν_0, is regarded as ergodic and therefore a fixed value. The distribution characteristics of random variables are stated in Table 1:

Variable	Unit	Description and distribution	Mean	C.O.V.
a_o	mm	Initial Crack Size (Moan, 1997) - Exponential	0.38	1.0
a_d	mm	Detectable Crack Size (MPI) Exponential	0.89	1.0
a_r	mm	Post-repair initial crack size Exponential	0.38	1.0
a_c	mm	Critical crack size Normal	15	0.04
lnC	$N^{-3}mm^{5.5}$	Material parameter Normal*	-29.97	0.017
lnC_r	$N^{-3}mm^{5.5}$	Post-repair material parameter Normal*	-29.97	0.017
lnA	MPa	Weibull scale parameter Normal**	1.6	0.138
$1/B$	-	Weibull shape parameter Normal	1.25	0.1
m	-	Material parameter Fixed	3.1	-
ν_0	Year	Annual stress cycles Fixed	$6.0 \bullet 10^6$	-
d	mm	Plate thickness Normal	50.0	0.04
Y_1	-	Geometry parameter 1 Lognormal	1.0	0.2
Y_2	-	Geometry parameter 2 Lognormal	2.0	0.1
ΔK_{th}	$Nmm^{-3/2}$	Stress intensity range threshold Fixed	0	-
K_{cr}	$Nmm^{-3/2}$	Fracture toughness Fixed	2.315	-
σ_{max}	MPa	Critical stress value Fixed	290	-

Table 1: Stochastic model for FM calibration
(c.o.v. = Coefficient of variance = s.d./mean; $\log(x) = ln(x)/ln(10)$)

A semi-elliptical surface flaw in a plate with a finite width of 400mm and a thickness d of 50mm is assessed. The surface defect is assumed to initiate from the centre of the plate and grows with a constant aspect ratio $a = 0.50$. Geometry effects for this particular crack are accounted for by a simplified Raju and Newman geometry function (Jiao and Moan, 1990; Madsen et al., 1987 and Tvedt, 2006).

$$Y(a,d) = exp\left\{Y_1\left(\frac{a}{d}\right)^{Y_2}\right\} \quad [5]$$

Failure is defined by the exceedence of the critical crack length a_c based on instantaneous fracture, where σ_{max} is the maximum stress value that should be related to the wave with a return period equal to the lifetime (Kaminski et al 1993):

$$a_c = \frac{1}{\pi}\left(\frac{K_{cr}}{Y(a,d)\cdot\sigma_{max}}\right)^2 \quad [6]$$

Note that this example is limited to cyclic loading and that constant loads and residual stresses are bound to be present and should be taken into account for the estimation of the critical crack size. The time-dependent limit states are evaluated with the use of probabilistic analysis software (DNV Sesam Probability) and non-linear programming is deployed to determine design point $\mathbf{u}^*$, as this method provides better stability compared to the Rackwitz-Fiessler algorithm (DNV, 2004). The calculation of conditional probability is performed by analysis of intersections with multivariate normal distribution methods.

Although the First Order Reliability Method (FORM) is considered less favourable for structural reliability research due to limited accuracy (Lee, 2012) and flexibility (Song, 2008), several studies on the use of FORM in fatigue fracture reliability validated with Monte Carlo simulations (Lee and Song, 2012 and Shabakhty, 2004) show that analytical approximation methods have appropriate accuracy. The sensitivity of β to changes in random variables χ are formulated with $\Delta\chi$ as the relative change of the mean value of χ and the variable lnC is concluded to be dominant, followed by the loading variables lnA and B, and remain stable over time.

Inspection Scenarios

The PoF conditioned on the results of a single inspection is calculated with the bivariate normal probability approach and a no-detection inspection restores the reliability index above the original curve (Ayala-Uraga and Moan, 2002 and Tvedt, 2006), because the non-existence of a crack implies conservative input of the initial curve:

$$P_{f,up} = P[M(\mathbb{x},t) \le 0 | IE_{nd}(\mathbb{x},T_{in}) > 0] \quad [7]$$

Figure 1 displays the no-detection updating for different inspection methodologies and inherent -qualities and the annual reliability index β. For advanced methods, with a small a_d, the amount of reduced uncertainty clearly is higher than for less-advanced methods.

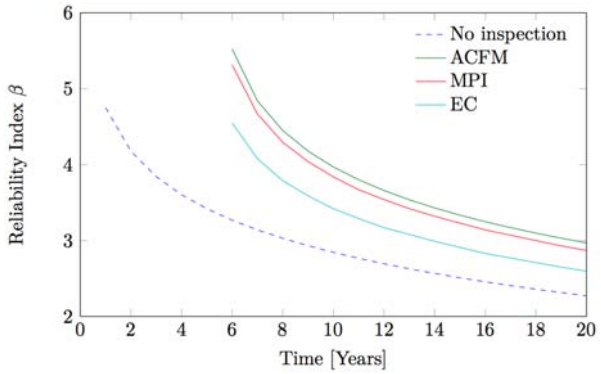

Figure 1: Inspection updating for different inspection methods

Eddy Current inspection reduces the epistemic uncertainty less than Magnetic Particle Inspection or Alternate Current Field Measurement. An *ideal* inspection, with $a_d = 0$, would eliminate all epistemic uncertainty and would lift the updated reliability curve extremely high. This theoretical case will not occur in real structures, for two reasons: the non-ideal inspection accuracy is inherent to inspection equipment and human interpretation, and the presence of initial surface defects, at least at welded joints.

The conditional reliability after detection and repair are defined and depicted through subjoined Equation 8 and Figure 2:

$$P_{f,up} = P[M_r(\mathbb{x},t) \le 0 | IE_d(\mathbb{x},T_r) = 0] \quad [8]$$

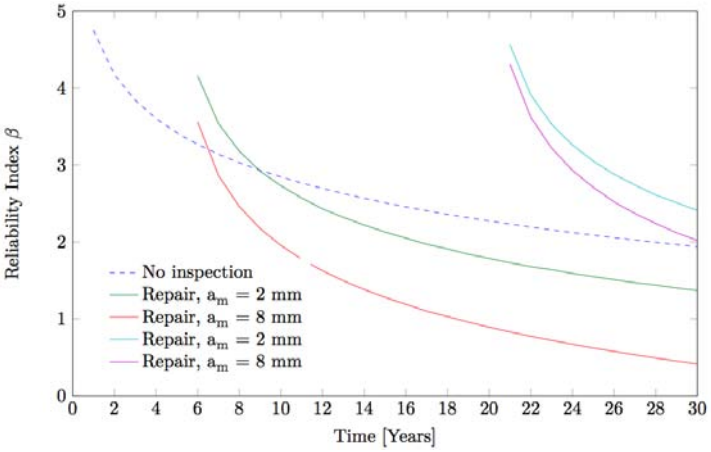

Figure 2: The conditional reliability after the detection and repair

It is seen that the repair initially lifts the reliability index above the original curve, because despite the existence of the crack, the component has a substantial amount of capacity remaining. The steepness of the updated reliability curve is a function of the repaired crack size; decline similar to the original curve for small cracks, and a steep decline for large cracks. The existence of a substantial crack implies a more rapid crack growth than implicit in the initial conditions (Tvedt, 2006), and updates the limit state function M_r in an unfavourable way (Moan and Song, 2000). However, if the same crack size is found at a later moment in time, the updating is much less unfavourable. This also can be observed in Figure 2; the detection of an 8 mm crack at 5 years causes a rapid decline of reliability, while the same detection at 20 years updates the reliability far more positive. As the original reliability curve models deterioration, the expectation of crack detection increases in time.

A very early damage detection will therefore update the original curve more negatively than crack detections at a later stage. Subsequently, detection followed by no-repair are defined and depicted through subjoined Equation 9 and Figure 3:

$$P_{f,up} = P[M_{nr}(\mathbb{x}, t) \leq 0 | IE_d(\mathbb{x}, T_m) = 0] \quad [9]$$

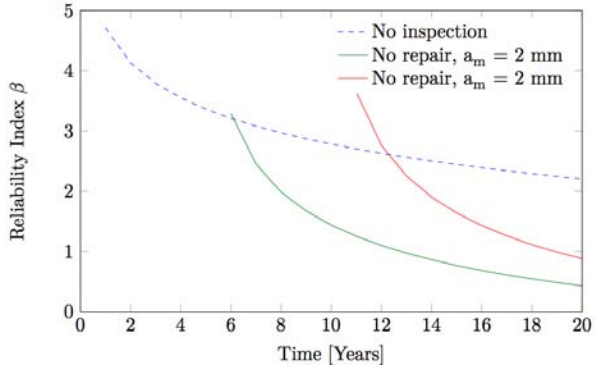

Figure 3: Inspection and no-repair after 5 and 10 years

It is seen that small cracks might initially lift the reliability due to remaining fracture resistance of the component, however this rapidly declines. Early crack detection will result in a more negative updating compared to later crack detections, similar to Figure 2. Logically, ship and offshore structures feature multiple inspection scenarios and outcomes in time. Hence, subjoined Equation 10 describes two consecutive no-detection inspection outcomes:

$$P[M(\mathbb{x}, t) \leq 0 | IE_{nd}(\mathbb{x}, T_1) > 0 \cap | IE_{nd}(\mathbb{x}, T_2) > 0] \quad [10]$$

It is found that inspection updating with the complete inspection outcome history result provides identical results as updating with only inspection outcome T_2. Limit states $IE_{nd}(T_1)$ and $IE_{nd}(T_2)$ depend on the same random variables $\mathbb{x}$ and therefore have almost identical failure surfaces and vectors α. Consequently the correlation $p = \alpha_1 \alpha_2^T$ will be extremely high. This implies that the information overlap between the two inspection outcomes is considerable and a single inspection is sufficient for updating. This implies that an inspection history with combinations of detection and no-detection outcomes cannot be described with only the last inspection, as the correlation $p = \alpha_1 \alpha_2^T$ is lower. It is known that reliability updating with the inspection history differs from updating with only the latest inspection information if no detections are made at T_1 and a crack is found at T_2 or another subsequent moment. However, the simplification described above reduces the number of intersections in calculations of Equation 10 and thereby reduces calculation effort (Ayala-Uraga and Moan, 2002). In general, it may be assumed that temporal correlation between inspection events decreases with time. Subjoined Figure 4 shows the curve for a fully independent a_d lifted above the dependent a_d.

Summarizing the above, it can be concluded that:

- Inspection history is only relevant if the history holds a combination of detection and no-detection outcomes. However this implies full dependency of the detectable crack size in $IE_{nd}(T_1)$ and $IE_{nd}(T_2)$. Which is arbitrary as inspection quality is influenced by the deployed methodologies and human- and environmental factors;
- In the evaluation of the limit states, the reliability index showed most sensitive to loading and material parameters, while less sensitive to initial and critical crack sizes;
- The method used to detect cracks, and the associated mean detectable crack size a_d, has considerable influence on the updating effect;
- The moment of detection has a high influence on reliability updating;
- Early crack detections update the original reliability far more negative than later crack detections;
- Inspection history has a limited effect on updating efficiency, as long as no cracks are found. However, if crack detections are present in the inspection history, reliability should be conditioned on all inspection outcomes.

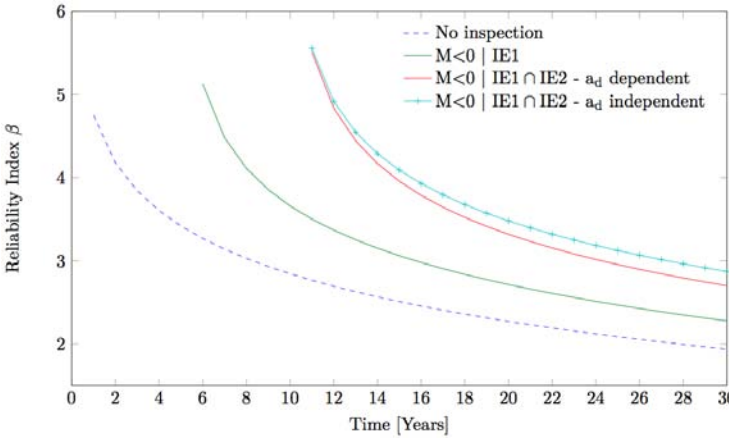

Figure 4: Inspection updating with dependent- and independent a_d

Inspection updating of System Reliability

To reflect real-life situations, the methodology has to be extended to system level, which is complicated by the complex relations between the various component limit states. Spatial correlation (in material properties and load mechanisms) is often neglected in structural deterioration models, while it is recognised that such an approach does not provide very accurate reliability estimations (Vrouwenvelder, 2004 and Straub, 2004). Spatial correlation is also considered to be relevant if one wants to draw conclusions about individual components based on system information (Moan and Song, 2000). Furthermore, variation in time also affects inspection conclusions as well. If a structure is simplified as a series system, each component failure results in system failure. Subsequently, the fatigue fracture growth of individual component n can be described by the limit state function [11], with $\mathbb{x}_n$ as the vector of the random variables describing the component.

$$M_n(\mathbb{x}_n, t) = \int_{a_{0n}}^{a_{cn}} \frac{da}{(Y(a)_n \sqrt{\pi a})_n^m} - C_n T \nu_n A_n^{m_n} \Gamma \left(1 + \frac{m_n}{B_n}\right) \quad [11]$$

If in a system with n components all vectors $\mathbb{x}_n$ are regarded as independent, as well are the events $M_n(\mathbb{x}_n, t)$. For this special situation the system PoF is simplified to the sum of all component failure probabilities. Hence, system reliability decreases with the number of components. For structures modelled as parallel systems, reliability increases with the number of components. Hence, the product of component reliability can describe system failure probability, if random variables $\mathbb{x}_n$ are independent. However, if the random variables between individual components are not independent, but to a certain degree correlated, calculation of system reliability requires a multi-normal approach.

Before the role of spatial correlation on system reliability can be investigated, the source and physical meaning needs to be known. Several types of correlation can be identified:

I. Material correlation is present due to shared material properties and environmental conditions for a (sub)structure, such as steel details and corrosion (protection). Specification requires testing, but it may is reasonable to assume some degree of correlation;
II. Loading correlation is relevant if components in a (sub)structure are subjected to equivalent load mechanisms. Strong load correlation is to be expected if different hotspots are subjected to a shared load mechanism, e.g. different hotspots in the same tubular detail subjected to wave-induced bending;
III. Initial defect correlation is caused by the dominant use of welding and the related similarities of weld type, material, procedures and welding conditions across different joints.

The general correlation structure based on the points above is shown in the matrix [12]. The diagonal axis shows direct correlation between similar random variables, such as $\rho A_i A_j$. Correlations outside the diagonal, e.g. $\rho C_i, a_{c,j}$ may have physical backgrounds as random variables are a function of material properties and environmental conditions (BS7910, 2005). Correlation between lnA and B is mentioned in several publications (Tvedt, 2006 and Madsen and Sorensen, 1991) and originates from the methods used to find the Weibull parameters given a certain long-term stress distribution.

$$R_{i,j} = \begin{array}{c|ccccc} & a_{0_i} & a_{c_i} & C_i & A_i & B_i \\ \hline a_{0_j} & \rho & 0 & 0 & 0 & 0 \\ a_{c,j} & 0 & \rho & \rho & 0 & 0 \\ C_j & 0 & \rho & \rho & 0 & 0 \\ A_j & 0 & 0 & 0 & \rho & \rho \\ B_j & 0 & 0 & 0 & \rho & \rho \end{array} \quad [12]$$

Independency in $R_{i,j}$ implies the non-existence of a physical relation between random variables. It is assumed that loading variables A and B are not correlated to material or fracture growth variables. Also the initial crack size a_0, related to fabrication and wear, is modelled as independent from all other variables.

In subjoined Figure 5, the system reliability for various degrees of correlation is displayed. For simplicity, the degree of correlation is taken equal for all random variables in $\mathbb{x}$. By increased correlation between different components, the system reliability tends to the value of single component (Moan and Song, 2000), as can be observed. Consequently, neglect of correlation is conservative for series system, while it is non-conservative for parallel systems. Conclusions about the effect of correlation on system reliability are not at all original (Thoft-Christensen, 2004), but the implications of correlation on inspection updating of structural systems has not received much research attention.

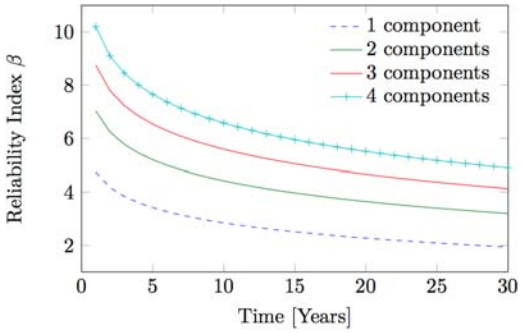

Figure 5: Reliability of a 3-component parallel system with a varying degree of general correlation between $\mathbb{x}_1$, $\mathbb{x}_2$ and $\mathbb{x}_3$

Foregoing, it was stated that inspection history becomes irrelevant if sequential inspections have similar results, but only if the PoD is dependent. In this model, it is assumed that no change of material- or load parameters occurs before and after the inspection. Since propagation into new material is inherent to crack growth, this simplification might not be realistic. Vrouwenvelder (2004) states that there is no reason to assume that C changes in the course of time, but on the other hand there is no guarantee that C is constant along the crack. For small cracks this effects is expected to be less important than for more substantial manifestations or when propagating through multiple components. Inspection updating will be more effective if C is stronger correlated in the period before and after the inspection, idem for load parameters A, B and v_0. For systems under ideal inspection, system reliability can be updated analogous. Two mathematically different ways are pursued. Firstly, the updating of each component with only the accessory inspection information:

$$P_{sys,up} = P\left[\bigcap_{i=1}^{n}(M_i(t) \le 0 | IE_i\right] = \quad [13]$$

$$\frac{P[\bigcap_{i=1}^{n}(M_i(t) \le 0 \cap IE_i]}{P[\bigcap_{i=1}^{n}(IE_i)]}$$

or updating of each component with all available information D:

$$P_{sys,up} = P\left[\bigcap_{i=1}^{n}(M_i(t) \le 0 | IE_i\right] = \quad [14]$$

$$\frac{P[\bigcap_{i=1}^{n}(M_i(t) \le 0 \cap IE_{sys}]}{P[\bigcap_{i=1}^{n}(IE_{sys})]}$$

Although the two approaches appear to be different, they are mathematically equivalent in the case of ideal inspection. The similarity of the methods suggests that inspection information of the component itself is extremely dominant, and the influence of other components may be neglected (Moan and Song, 2000). This is due to the high degree of correlation between failure event M_i and inspection event IE_i, caused by the shared random variables. In Figure 6 it is shown that, despite high correlation between M_i and inspection information of other components, IE_j and IE_k, no considerable increase in reliability updating occurs.

The small increase is assigned to the independent modelling of the detectable crack size a_d.

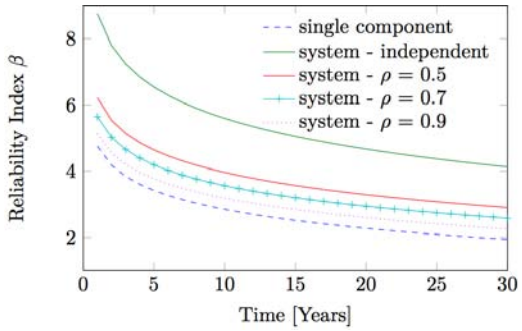

Figure 6: Reliability of a single component based on different amounts of no-detection information, correlation between component variables ρ = 0.9

System Updating with Non-Ideal Inspection

As mentioned, the scope of real-life inspections on ship and offshore structures are incomplete by nature, due to:

- Prescribed inspection procedures;
- Operation-dependent accessibility of subsystems;
- Weather-dependent accessibility of subsystems;
- Inspection costs.

Despite missing information about certain components, knowledge can be gained about these uninspected parts, due to the presence of structural correlation. Consequently, system reliability can be updated based on partial inspection information. This statement is clarified in the next two sections.

Updating of Uninspected Components with System Inspection

Before the effect of the extend of partial inspection is investigated, the updating of uninspected components with system information is addressed. For systems with low correlation, with $\rho = 0.5$, the reliability curve is lifted only slightly above the original. For higher correlation between the components, reliability is updated higher, but the difference in updating results between inspection extend is not as large. For both levels of correlation, it can be concluded that neglect of correlation between component limit states results in conservative reliability estimations of the uninspected component, if no cracks are detected.

If the system inspection information includes crack detection, the uninspected joint is updated in a negative way, as seen in subjoined Figure 7. In this case, IE_j is the detection of a 5mm crack. With the incorporation of the no-detection event, the system information is used for updating. In IE_k and IE_j, the negative effect is slightly less. It can be seen that neglect of the system information results in non-conservative reliability estimation of the uninspected joint if crack detections are made.

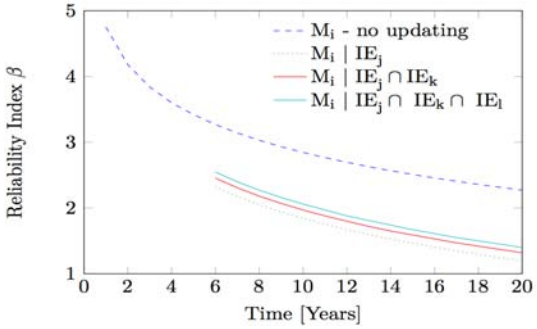

Figure 7: System updating of uninspected component, if IE_j is a detection of 5mm, $\rho = 0.5$

Updating of Systems with Incomplete Inspection Information

To investigate the effect of inspection extend, a simple parallel system with 4 components with equal β-indices is modelled. Inspection of varying extend is conducted at $T = 5$ years with no crack detected. Figure 8 displays the outcome for a highly correlated system. As expected, the effect of reliability-updating increases with inspection extend. In addition, merely one single inspection updates the reliability by a considerable amount, while the inspection extension contributes less.

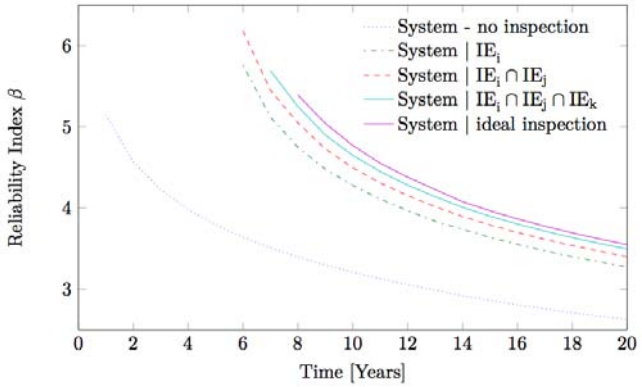

Figure 8: Reliability of a 4-component parallel system, updated with different inspection extend. Correlation between component variables ρ = 0.9

In Figure 9, the cumulative updating effect at $T = 12$ years, for the same parallel 4-component system, is presented as a function of correlation between components. For low correlations, $\rho = 0.5$, a single component inspection already obtains 50% of the maximum available information, and every increase of inspection extend has a considerable updating effect. For high correlation is can be concluded that an inspection extend of three components accounts for ±90% of the reliability updating, and an ideal inspection would add little extra information.

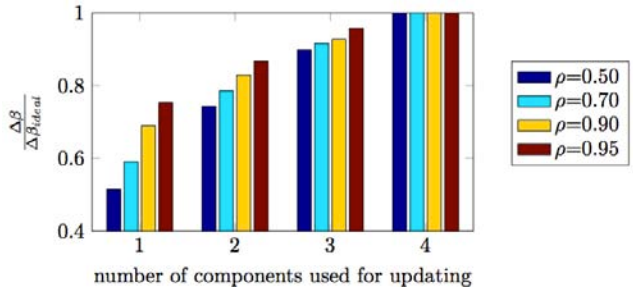

Figure 9: Updating efficiency as a function of inspection extend, for a 4-component parallel system at T = 12 years

To summarize, the effects of correlation on system reliability are dominant in both system reliability estimation and inspection updating. On component level, disregard of correlations results in conservative reliability estimations for non-inspected components as long as no cracks are detected. Vice-versa, non-conservative if crack detections are made. This strengthens the idea that inspection strategy should focus on the most critical components if a limited number of components are inspected (Moan and Song, 2000) and underlines the relevance of the use of correlation in system updating and RBI-practices. From reliability perspective an ideal inspection has small added value over a partial inspection if correlation between components is high, because inspection-updating efficiency is a function of both inspection extend and system correlation.

Although FORM is considered suitable for the evaluation of inspection updating for single component scenarios, for system-description the method may not be the optimal solution, as the complexity of calculation of multivariate normal distributions limits the number of intersections that can be evaluated. In addition, structural reliability is often modelled by a combination of series and parallel systems (Ditlevsen and Madsen, 1996).

It is noted that this approach neglects the effect of local load updating, that seems relevant for fatigue fracture failure (Shabakhty et al., 2003 and Karamachandani et al, 1991). Fatigue failure should be described by analysis of sequential failure, in which the description of component limit states depends on the previous component failure (Lee and Song, 2012 and Kurtz et al., 2012).

A key challenge in the utilisation of structural correlation now becomes the approximation of correlation for all the relevant random variables. Of all these variables, it is expected that correlation in material and initial defects variables can only be based on empirical data. Very limited research attention has been given to this topic. Vrouwenvelder (2004) introduced a general spatial correlation of ρ = 0.85, based on small scale experiments and theoretical research, but no validation of this estimation has been performed. Moreover, NORSOK standard N-006:2009 states "*The reliability of a considered detail can alternatively be controlled by in-service inspection of areas with strongly correlated loading close to the considered hot spot.*" This strengthens the idea that load variables can be approached in a theoretical way.

Load Correlation Case Studies

As stated, the key challenge in the application of system updating lies in the correct estimation of correlations. Effort should focus on loading and material correlation as these were found to be dominant in the calculation of the reliability index. In guidelines for the assessment of ship and offshore structures, the use of information from surroundings details for assessment of uninspectable joints is mentioned (NORSOK, 2009). However, no specific methodology is proposed. Hence, a method for the approximation of load-correlation based on variance of the stress processes in short term sea states is proposed with a (limited) case study for illustration. Different fatigue-prone locations platform are investigated to define the correlation between the different locations.

Firstly, the calculation of load correlation is performed in four steps:

1. Generate irregular sea states for the asset location;
2. Calculate stress transfer functions with a time domain analysis of stress responses;
3. Calculate short term stress distributions for the relevant sea states;
4. Obtain correlation coefficients based on variance of short term wave spectra.

Wave force is the dominant load mechanism for fatigue damage of both substructures, so no attention is given to wind and current loads. A Pierson-Moskovic energy density spectrum is used to describe irregular waves, as small waves dominate the fatigue fracture growth for this case. The probability of a certain sea state with a combination of significant wave height H_s, mean zero-upcrossing period T_z, and dominant wave direction θ is obtained from the normalized direction wave scatter diagram available for the location. An irregular sea state is generated as a superpositioning of regular waves. The amplitudes ζa for each regular wave can be determined knowing that the area under the associated segment of the spectrum, $S\zeta\ (\omega)\ \cdot\ \Delta\omega$, is equal to the variance of the wave component (Journée and Massie, 2001). Each regular wave is assigned with a random seed to prevent unrealistic interference during the start of the irregular wave trace. Next, the wave loads on the circular legs are approximated with the Morison equation (the sum of the inertia and drag forces) and the time trace of velocities and accelerations are obtained with linear wave theory equations (Journée and Massie, 2001).

The transfer function describes the frequency dependent relation between waves of a certain sea state and the associated stress at a certain location. Dynamic Time Domain Analysis software is used to solve the equations of motion of a finite element model of the asset in the time domain in response to given environmental loads. Output of the program includes a time record of internal forces and moments at requested locations in the structure. The time record of stress at a certain location is obtained by multiplication of internal forces and moments with stress operators and a Fourier transform of the time record results in the frequency spectrum of the stress process. Finally, the sea spectrum is used as input for the wave forces is regenerated to obtain the transfer function.

Wave height in a short-term seastate is Rayleigh distributed if the water surface elevation is a narrow banded Gaussian process (Journée and Massie, 2001). The same distribution type can be used for the description of the wave-induced stresses, as long as a linear relation between wave height and stress amplitude is assumed. This linear relation might not be valid for all wave heights, but since the majority of the fatigue damage is expected to be caused by small waves, the simplification is considered adequate. The total number of stress cycles in a short term sea state is a function of the mean zero-upcrossing period T_z, σ, and the probability density of that particular sea state is determined through:

$$N_{shortterm} = \frac{T_{total}}{T_{z,\sigma}} \cdot O(H_z, T_z, \theta) \quad [15]$$

$$T_{z,\sigma} = 2\pi \sqrt{\frac{m_{2\sigma}}{m_{0\sigma}}} \quad [16]$$

With $O(H_z, T_z, \theta)$ as the normalised directional wave scatter diagram. The occurence of stress within a certain bandwidth can then be calculated with superpositioning of the number of oscillations of ΔS within all short term sea states:

$$N_{longterm}(\Delta S) = \sum_{\theta} \sum_{H_s} \sum_{T_z} \left(N_{shortterm}\ (H_z, T_z, \theta) \cdot \frac{\Delta S}{m_{0\sigma}(H_z, T_z, \theta)} \cdot exp\left\{ \frac{\Delta S^2}{2 \cdot m_{0\sigma}(H_z, T_z, \theta)} \right\} \right) \quad [17]$$

The long-term distribution of stress is assumed to follow a two-parameter Weibull distribution (Skjong et al., 1995). Weibull scale and shape parameters A and B can be found with linear regression; by re-arranging the cumulative probability function of the stress $F(S)$:

$$F(x) = 1 - \exp\left(-\frac{S}{A}\right)^B \ln\left(\ln\left(\frac{1}{1 - F(S)}\right)\right) = \quad [18]$$

$$B \ln(S) - B \ln(A)$$

Case I: Leg 2 at Tank Level

The first case study investigates load correlation between different locations in a tubular section of leg 2 of the 3-legged platform. The cross section is modelled with 8 different fatigue fracture locations and assessed at the caisson tank roof level. Based on the distribution of stresses over the circumference, it is expected that locations 180° apart will be extremely high correlated, while locations 90°apart will lower correlated.

For each hotspot, 12 directional transfer functions, ranging from $\theta = 0°$ to $\theta = 330°$, are obtained and transfer functions for hotspots 21001 and 21003 for wave directions $\theta = 0°$ to $\theta = 90°$ are constructed. With all transfer functions available, the stress spectra for each combination of wave height, wave period and wave direction can be generated. The zero-order moment of the stress spectra, $m_{0\sigma}$, can be used as a measure for the expected stress-value in a particular seastate. Correlation is then established by comparing $m_{0\sigma}$-values, corrected for the probability of a particular seastate, between different hotspots.

In Figure 10, the stress correlations between the 8 locations in leg 2 at tank level are presented. The associated Pierson correlation coefficients can be found in Table 2. As expected, the correlation between opposite locations, e.g. 21001 and 21005, is extremely high. Correlation found between hotspots with a 90◦ shift, e.g. 21001 and 21003, remain substantial. However, lower relative to the overall correlation in the tubular section. Within the illustrated scatter of the subjoined figure, some clustering for certain wave directions can be observed. This leads to the believe that within the total stress response, the responses for some wave directions are more correlated than for other wave directions.

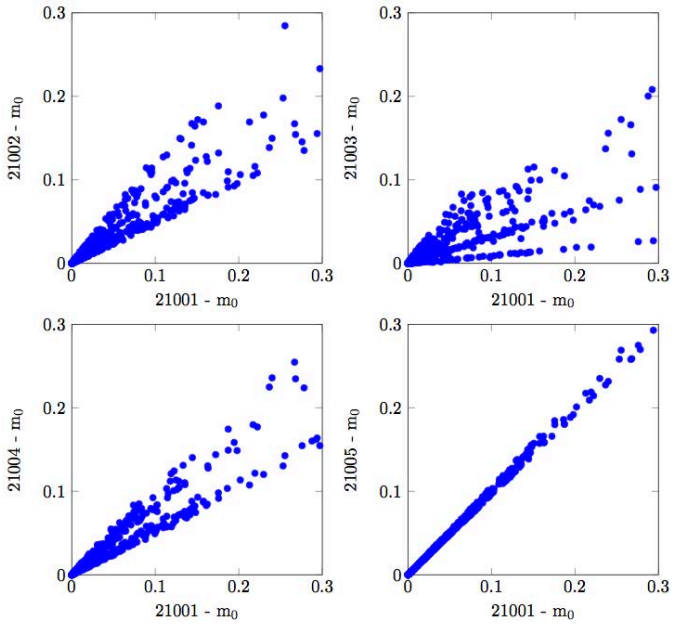

Figure 10: Correlation between first-order moments of short-term stress spectra, corrected for probability of the associated sea state

Hotspot	21001	21002	21003	21004	21005	21006	21007	21008
21001	1	.9348	.8499	.9619	.9993	.9239	.8508	.9552
21002		1	.9070	.8557	.9459	.9994	.9074	.8519
21003			1	.8816	.8522	.9144	1	.8901
21004				1	.9527	.8465	.8824	.9995
21005					1	.9355	.8531	.9457
21006						1	.9148	.8436
21007							1	.8909
21008								1

Table 2: Stress process correlation leg 2 (21001-21008), at tank level

Case II Leg 2 and Leg 3 at Tank Level

Correlation between a section of leg 2 and leg 3, at tank level, is assessed in case II. The sections have identical geometry and stress operators, but different transfer functions. Therefore, the stress will not be fully dependent. The next figure displays the correlations between hotspot 21001 and various locations in leg 3 (again the associated correlation coefficients are displayed in Table 3).

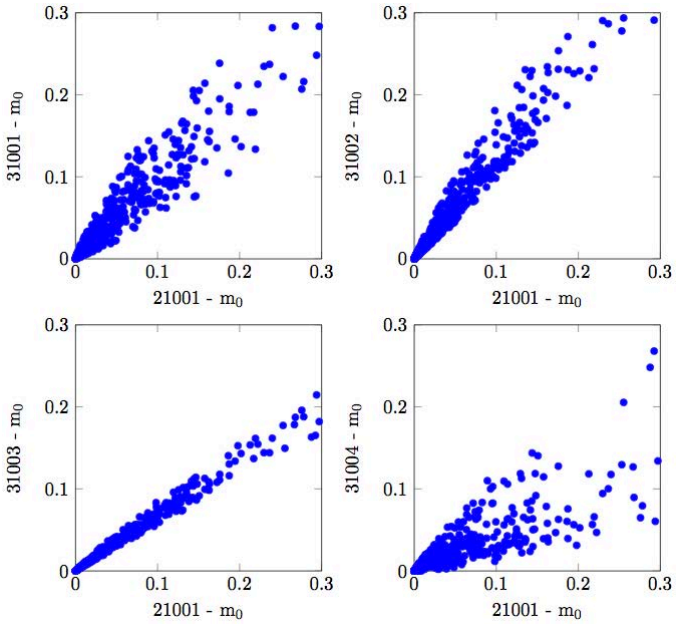

Figure 11: Load correlation between leg 2 and 3, at tank level

Hotspot	21001	21002	21003	21004	21005	21006	21007	21008
31001	.9636	.9699	.9361	.9353	.9671	.9673	.9367	.9339
31002	.9865	.9075	.8430	.9643	.9838	.8966	.8441	.9585
31003	.9945	.9163	.8144	.9503	.9934	.9035	.8152	.9419
31004	.8537	.9736	.9284	.7875	.8675	.9795	.9280	.7883
31005	.9567	.9753	.9428	.9257	.9612	.9738	.9434	.9248
31006	.9865	.9139	.8518	.9639	.9842	.9036	.8529	.9584
31007	.9933	.9094	.8077	.9508	.9917	.8961	.8085	.9423
31008	.8526	.9724	.9299	.7880	.8662	.9783	.9295	.7889

Table 3: Stress process correlation between 8 hotspots in a tubular section

Besides the higher correlation between locations 21001 and 31003, which are oriented in the same direction and therefore related to the sway motion of the platform, high correlation is observed between locations 21001 and 31002. This is explained by the rotational mode shape of the platform, caused by the uneven distribution of leg stiffness in the platform's longitudinal direction (a second peak, at $\omega = 1.5\ [rad/s]$, is observed for location 21001).

The cases show a very high level of general correlation. This can be explained by the similarity in dominant load mechanism and the identical geometry. It is noted that the method's application hinges on the correct assessment of the stress operators. In context with the aforementioned statement on the use of loading correlation for uninspectable (NORSOK, 2009), a key challenge in system inspection updating is the determination of the best location for inspection. Which is, as mentioned, analogous to Risk Based Inspection practices.

In essence, RBI-equivalent considerations and decisions need to be made regarding the optimization of system reliability for partial inspection scenarios:

- Inspection frequency. Hence: '*How often to inspect?*' With a target reliability values in place, the time to the next inspection can be determined based on the last inspection results, or the whole inspection history (if relevant). In this way, the cost and inherent risks of inspections are reduced, while adequate levels of reliability are maintained;
- Inspection extend: '*How many locations to inspect?*' Operators need to inspect a number of locations, as required by rules and regulations. With quantified correlation knowledge, the number of locations to inspect can be determined in a rational way, balancing cost and reliability;
- Inspection location: '*Where to look for damage?*' If correlation between the crack growth of individual components is quantified, the knowledge gained from a partial inspection can be estimated. In this way, operators are able to compare different spatial inspection proposals and balance costs for the optimal inspection practice.

In this paper, no attempts are made to touch upon the subject of Risk Acceptance Criteria; the product of probability of failure and its consequence, which results in a target value of β that needs to be maintained during the structural lifetime. DNV provides with acceptable annual failure probability as displayed in the subjoined table 4.

Class of Failure	Consequence	
	Less serious	Serious
I. Redundant structure.	$P_f = 10^{-3}$	$P_f = 10^{-3}$
	$\beta = 3.09$	$\beta = 3.09$
II. Significant warning prior to occurrence in a non-redundant structure.	$P_f = 10^{-3}$	$P_f = 10^{-3}$
	$\beta = 3.09$	$\beta = 3.09$
III. No warning prior to occurrence in a non-redundant structure.	$P_f = 10^{-3}$	$P_f = 10^{-3}$
	$\beta = 3.09$	$\beta = 3.09$

Table 4: Acceptable annual failure probability and target reliability index

The target values of DNV are applied to the example of component updating with non-ideal inspection information. In Figure 11, two different target values for redundant structures are displayed. The level of loading correlation found in this chapter, and the earlier mentioned correlation in material parameter C, are applied. No-detection inspection information of $T = 5$ years is used.

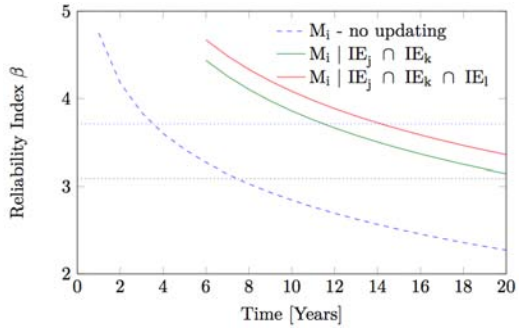

Figure 11: Effect of different β-targets; β = 3.71 (blue line) and β = 3.09 (black horizontal dotted line)

For the high target value, the inspection at $T = 5$ years is overdue, as the target value is not maintained. For the low target value, inspection is required just before the 8th year. The inspection updating is effective for maintaining the target reliability for the high target value. Also, the effect of the inspection extend on the required inspection interval can be seen; if inspection information of three components is used the inspection interval is extended with 2 years, compared to the two-component inspection. For the low target value, no second inspection is required for an adequate level of reliability.

CONCLUSIONS

It is concluded that reliability measures are most sensitive to load and material variables and the accurate assessment of these uncertainties is challenging and relevant for further research into spatial en temporal correlation. These difficulties are a common reason to refrain from reliability methods, while they should not give reason for abandonment of the method, as in essence they merely introduce epistemic uncertainty, which are not fundamentally different from uncertainties already present in the approach.

For the single component fatigue fracture model it was found that the inspection method, and associated Probability of Detection curve, has considerable influence on reliability updating results. Also, inspection history showed little effect on updated reliability as long as no crack detections are made. However, if cracks are detected, reliability should be conditioned on the complete inspection history. Hence, the central conclusion of this paper comprises the role of correlation in system reliability: spatial and temporal correlations are highly relevant for both system reliability estimation and updating. Disregard of structural correlation results in misunderstanding of system reliability and inefficient use of system inspection information. On the component level, neglect of correlation misjudges reliability of un-inspected components if system inspection information is available.

Note that in no way the probabilistic Fracture Mechanics-approach to fatigue deterioration should be regarded as a substitute for the S-N approach. It merely is a strong alternative, advantageous for situations where decisions have to be based on damage. The probabilistic fracture growth model should be calibrated with rules and regulations, in an effort to enable the practical use of the method (Tammer et al., 2014).

Future perspective and challenges

The key challenge for structural engineers is to bridge the gap between the solid understanding of structural deterioration on material science level and practical models for assessment of complete structures. As an emerging methodology, Risk Based Inspection will claim an inevitable role in determining inspection intervals and cost optimization cases with respect to fatigue degradation of ship and offshore structures.

The methodological difficulties in the collection of accurate data and the determination of the total accumulated fatigue damage for specific locations can be enhanced through the application of structurally correlated inspection data. Therefore, it is recommended to direct additional research efforts into:

- Calibrating the probabilistic Fracture Mechanics model to the S-N approach to comply with rules and regulations;
- The assessment of fatigue fracture deterioration in conjunction with other failure modes, such as brittle fracture, corrosion or yielding;
- Address and research learning effects during inspection, as the Probability of Detection should be conditioned on the history of crack detection.

REFERENCES

Ayala-Uraga, E., and Moan, T. (2002) System reliability issues of offshore structures considering fatigue failure and updating based on inspection. 1st International ASRANet Colloquium, 8-10 July 2002, Glasgow, Scotland.

British Standards Institution (2005). BS7910:2005. Guide to methods for assessing the acceptability of flaws in metallic structures. London: British Standards Institution.

Det Norske Veritas, (2004/2005/2010). DNV-OS-C101. Design of Steel Offshore Structures, 2004. Recommended Practise C203 - Fatigue Design of Offshore Steel Structures, 2005. Classification Notes 30.7 - Fatigue Assessment of Ship Structures 2010. Oslo: DNV.

Det Norske Veritas. Proban theory v4.4. General Purpose Probabilistic Analysis Program (2004).

Demsetz, L. and Cabrera, J. (1999). Detection probability assessment for visual inspection of ships. Ship Structure Committee, SSC-408, Washington, D.C: USA.

Ditlevsen, O. and Madsen, H.O. (1996). Structural Reliability Methods. John Wiley & Sons. ISBN: 978-0471960867.

Health And Safety Executive (2002). HSE-OTO 2000/018. Offshore Technology Report 200/018 – POD/POS curves for non-destructive examination [Prepared by Visser Consultancy Limited, Visser, W.] HSE, Norwich: UK.

ICON database (1996) Inter-Calibration of Offshore Non-destructive testing.

Jiao, G., and Moan, T. (1990). Methods of reliability model updating through additional events. Structural Safety, pp. 139–153.

Journée, J., and Massie, W. W. (2001). Offshore Hydromechanics [reader]. Delft University of Technology (TU-Delft): The Netherlands.

Kaminski, M.L., Boonstra, H., Salza, P. and Wittenberg, L. (1993). Cost effective life-cycle design of semi-submersibles based on probabilistic fatigue calculations. In proceedings of the 12th International Conference on Ocean, Offshore and Arctic Engineering (OMEA). The American Society of Mechanical Engineers (ASME). Glasgow, UK.

Karamachandani, A., Dalane, J., and Bjerager, P. (1991). Systems reliability of offshore structures including fatigue and extreme wave loading. Marine Structures vol. 4, issue 4, pp. 353-379.

Kurtz, N., Song, J., Ok, S., and Kim, D. (2012). System reliability analysis of fatigue-induced, cascading failures using critical failure sequences identified by selective searching technique. Applications of Statistics and Probability in Civil Engineering [Edited by K . Nishijima]. pp. 1733-1740. CRC Press 2011 ISBN: 978-0-415-66986-3.

Lee, Y.J. (2012) Finite-element system reliability analysis and updating of fatigue-induced sequential failures. [Dissertation].

Lee, Y., and Song, J. (2012) Finite-element-based system reliability analysis of fatigue-induced sequential failures. Reliability Engineering and System Safety vol. 108, pp. 131–141.

Madsen, H., Skjong, R., Tallin, A., and Kirkemo, F. (1987). Probabilistic fatigue crack growth anal- ysis of offshore structures, with reliability updating through inspections. Marine Structures Reliability Symposium 1987.

Moan, T., Hovde, G.O., and Blanker, A.M. (1993). Reliability-based Fatigue Design Criteria for Offshore Structures Considering the Effect of Inspection and Repair. In: OTC7189 - Proceedings of the 25th Offshore Tech Conference, (vol. 2) pp. 591–599. Houston, Texas: USA.

Moan, T., Vardal, O.T., Hellevig, N.C. and Skjoldli, K. (1997). In-service observations of cracks in North Sea jackets - a study on initial crack depth and pod values. Proceedings of the 16th OMAE Conference. Yokohama: ASME.

Moan, T., and Song, R. (2000). Implications of inspection updating on system fatigue reliability of offshore structures. Journal of Offshore Mechanics and Arctic Engineering, pp. 173–180.

Norsok (2009). N-006:2009 Assessment of structural integrity for existing offshore load-bearing structures. First edition. Lysaker: Norway.

Shabakhty, N. (2004) Durable reliability of jack-up platforms - The impact of Fatigue, Fracture and Effect of Extreme Environmental Loads on the Structural Reliability [Dissertation]. ISBN: 90-3700217-X.

Shabakhty, N., van Gelder, P., and Boonstra, H. (2003) Reliability analysis of jack-up structures based on fatigue degradation. Safety and Reliability - Safety and Reliability – Bedford & van Gelder (eds) © 2003 Swets & Zeitlinger, Lisse, ISBN 90-5809-551-7.

Skjong, R., Gregersen, E., E, C., Croker, A., Korneliussen, G., Lacasse, S., Lotsberg, I., Nadim, F., and Ronold, K. (1995). Joint Industry Project: Guideline for offshore structural reliability analysis: Examples for Jacket Platforms. DNV Technical Report no. 95-3204.

Song, J., and Won-Hee, K. (2008) System reliability and sensitivity under statistical dependence by matrix-based system reliability method. Structural Safety vol. 31, issue 2, pp. 148-156.

Straub, D. (2004). Generic Approaches to Risk Based Inspection Planning for Steel Structures [online PhD dissertation]. Institute of Structural Engineering, Swiss Federal Institute of Technology, ETH Zürich. Available from: http://e-collection.library.ethz.ch/eserv/eth:1550/eth-1550-01.pdf

Tammer, M.D., and Kaminski, M.L. (2013). Fatigue Oriented Risk Based Inspection and Structural Health Monitoring of FPSOs. Proceedings of the 23rd International Offshore and Polar Engineering Conference (ISOPE) pp. 438-449. Anchorage, Alaska, USA.

Tammer, M.D., Kaminski, M.L., Koopmans, M. and Tang, J.J. (2014). Current Performance and Future Practices in FPSO Hull Condition Assessments. Proceedings of the 24th International Offshore and Polar Engineering Conference (ISOPE). Busan, Korea. [IN PRESS].

Thoft-Christensen, C. Engineering Design Reliability Handbook (chapter 15). CRC Press, 2004. ISBN: 0849311802. Edited by: Nikolaidis, E. Dan M. Ghiocel, D.M. and Singhal, S.

Tvedt, L. (2006). Proban - Probabilistic Analysis. Structural Safety 28, pp. 150–163.

Vrouwenvelder, A.C.W.M. (2004). Spatial correlation aspects in deterioration models. Proceedings, 2nd International Conference on Lifetime-Oriented Design Concepts, Bochum, Germany.